

Original Paper

# Precipitation of Carbides during Tempering of Cr-Mo steels

Koreaki TAMAKI and Jippeï SUZUKI  
(Department of Mechanical and Materials Engineering)

(Received September 16, 1982)

Carbide phase changes in various Cr-Mo steels during tempering were investigated by means of X-ray analyses, electron microscopic observations and chemical analyses. Two sequences of carbide precipitation were recognized, viz., (1)  $M_3C \rightarrow M_2C \rightarrow M_{23}C_6$  or  $M_3C^*$ , and (2)  $M_3C \rightarrow M_7C_3 \rightarrow M_{23}C_6$ . The carbide reaction (1) occurred in such the Cr-Mo steels of relatively lower chromium content, while the carbide reaction (2) occurred in those of higher chromium content. In such the Cr-Mo steels of medium chromium content, the carbide reaction (1) and (2) occurred simultaneously. The carbide phase diagrams were proposed to describe the type of carbide reaction and the period of individual carbide precipitation for 12 types of Cr-Mo steels.

## 1. Introduction

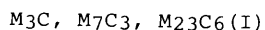
The behavior of carbide precipitation during tempering is one of the most important factors controlling the mechanical properties and the creep characteristics of heat treated Cr-Mo steels. Further, the authors indicated that the reheat cracking sensitivity of Cr-Mo steels was closely related to the carbide types precipitated during reheating, and suggested the mechanism of reheat crack initiation caused by the carbide in the previous paper<sup>1)</sup>.

The behavior of carbide precipitation in Cr-Mo steels is influenced not only by the individual alloying element, such as chromium and molybdenum but also by the mutual effect of their elements. Therefore it is required to investigate systematically the behavior of carbide in the steels with various Cr-Mo contents. In this paper, the carbide diagrams during tempering were shown for 12 types of Cr-Mo steels based on the experimental results of electrolytic extraction—X-ray analyses, electron microscopic observations and chemical analyses of extracted carbides using the specimens tempered at 500 to 700°C for 1 to 100 hours.

## 2. Previous works

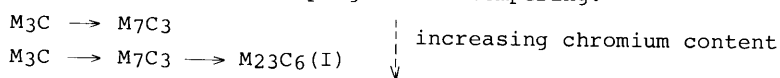
### 2.1 Chromium steel

K. Bungardt<sup>2)</sup> informed the cross section of Fe-C-Cr ternary equilibrium diagram at 700°C. The following carbides were formed in chromium steels as the Cr/C content ratio of the steel was increased under the equilibrium condition.



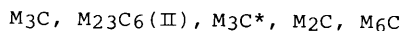
where the notation of  $M_3C$  represents the iron carbide,  $Fe_3C$  (Cementite) containing chromium as solid solution. Similarly  $M_7C_3$  and  $M_{23}C_6(I)$  represent the chromium carbides,  $Cr_7C_3$  and  $Cr_{23}C_6$  containing iron.

During tempering the quenched chromium steels, the following change of carbide phase occurred with the progress of tempering.<sup>3)</sup>



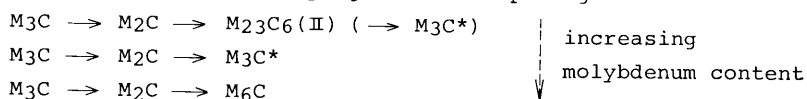
### 2.2 Molybdenum steel

T. Sato<sup>4)</sup> informed the cross section of Fe-C-Mo ternary equilibrium diagram at 700°C. The following carbides were formed in molybdenum steels as the Mo/C content ratio of the steel was increased under the equilibrium condition.



where  $M_3C$  represents  $Fe_3C$  containing molybdenum.  $M_{23}C_6(II)$  represents  $Fe_{21}Mo_2C_6$  containing iron as solid solution.  $M_3C^*$  was the Fe-Mo-C ternary carbide named  $\xi$ -carbide by T. Takei.<sup>5)</sup> And D.J. Dyson<sup>6)</sup> determined the stoichiometric formula,  $Fe_2MoC$  of  $\xi$ -carbide. In this paper the notation of  $M_3C^*$  was used for the representation of the iron-molybdenum carbide,  $Fe_2MoC$  containing iron in order to distinguish from the iron carbide,  $M_3C$ . The notation of  $M_2C$  represents the molybdenum carbide,  $Mo_2C$  containing iron. And  $M_6C$  represents the continuous series of solid solution between  $Fe_4Mo_2C$  and  $Fe_3Mo_3C$ .

During tempering the quenched molybdenum steels, the following change of carbide phase occurred with the progress of tempering.<sup>3)</sup>



As mentioned above,  $M_2C$  carbide followed after  $M_3C$  in all molybdenum steels. And then,  $M_2C$  carbide was changed to the final carbides corresponded to molybdenum content of steels.

### 2.3 Chromium-molybdenum steel

K.W. Andrews<sup>7)</sup> informed the cross section of Fe-Cr-Mo-0.12%C quaternary equilibrium diagram at 700°C, and W. Jellinghaus<sup>8)</sup> informed that of Fe-Cr-Mo-0.22%C. Carbide types present in quaternary system were same as those present in Fe-Cr-C and Fe-Mo-C ternary systems, and special quaternary carbide has not been recognized.

As concerned to  $M_{23}C_6(I)$  and (II), the authors assumed that  $M_{23}C_6(I)$  and (II) are mutually soluble in all proportion, because both the lattice structures are

the same and both the lattice constants are nearly the same. Then the single notation,  $M_{23}C_6$  was adopted for such the solid solution.

### 3. Materials and experiments

#### 3.1 Chemical compositions of steel specimens

8 kg ingots of various Cr-Mo contents were prepared by melting electrolytic iron and ferro-alloys in an induction furnace in the laboratory. Each ingot of 60 mm in diameter was forged into the steel bar of 16 mm in diameter. The following two series of Cr-Mo steels were selected based on the chemical compositions of HT80 steels and Cr-Mo heat resisting steels used currently, as shown in Table 1.

Series A : 0.5%Mo, 0 to 5%Cr

Series B : 1 %Mo, 0 to 4%Cr

Table 1 Chemical compositions of steel specimens (wt%)

No	C	Si	Mn	P	S	Cr	Mo
A-0	0.12	0.42	1.06	0.020	0.020	0.04	0.51
A-1	0.12	0.39	1.06	0.018	0.019	0.58	0.54
A-2	0.12	0.34	1.08	0.016	0.019	1.10	0.53
A-3	0.13	0.49	1.22	0.018	0.016	1.83	0.52
A-4	0.14	0.51	1.41	0.017	0.018	2.57	0.53
A-5	0.14	0.41	1.28	0.018	0.018	3.32	0.51
B-0	0.13	0.22	0.91	0.021	0.018	0.01	0.96
B-1	0.14	0.30	1.07	0.018	0.019	0.46	0.92
B-2	0.14	0.27	0.92	0.020	0.018	1.14	0.96
B-3	0.13	0.36	1.19	0.021	0.019	1.44	0.91
B-4	0.13	0.38	1.16	0.019	0.019	2.03	0.93
B-5	0.14	0.45	1.12	0.021	0.019	4.27	0.95

#### 3.2 Electrolytic extraction and X-ray analyses

Carbides were extracted electrolytically from the specimens quenched and tempered at 500 to 700°C for 1 to 100 hours using the electrolytic cell as shown in Fig.1. 0.5N HCl was used as electrolyte, and current density was 10 mA/cm<sup>2</sup>. Carbides as anode residue were filtered through a glass filter(G3). And then the filtrated carbides were washed by distilled water and ethyl alcohol, and dried in a desiccator.

X-ray diffraction with Cr target was carried out for the identifications of extracted carbides. Data cards published from JCPDS were used as the standard diffraction patterns.

When the specimen included two or more types of carbides, the weight fraction of the individual carbide was determined by following method. At first, the standards steel specimen, each of which contained mono type of carbide, was selected.  $M_3C$ ,  $M_2C$ ,  $M_7C_3$  and  $M_{23}C_6$  carbides were extracted from S45C(tempered at 600°C for 24 hours), 0%Cr-0.5%Mo(tempered at 700°C for 100 hours), 1.8%Cr-0.5%Mo(tempered at 600°C for 24 hours) and 4.3%Cr-1%Mo(tempered at 700°C for 100 hours)

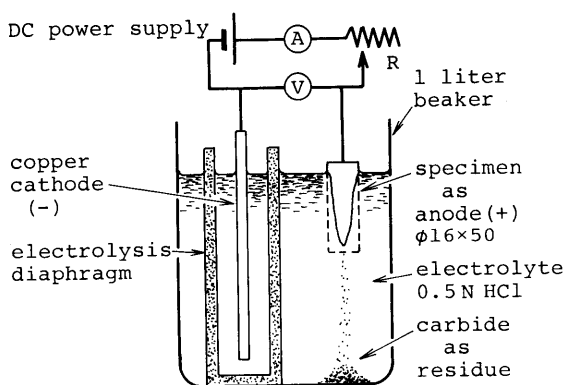


Fig.1 Apparatus for electrolytic extraction of carbides

respectively. Then these carbides were mixed artificially in proper weight fractions, and X-ray diffraction was carried out on such the carbide mixture. The calibration curves were made between the weight fractions of carbide and the intensity of diffracted beam. Fig.2 shows the calibration curves for the carbide mixtures of  $M_3C-M_2C$ ,  $M_2C-M_7C_3$  and  $M_7C_3-M_{23}C_6$ , respectively.

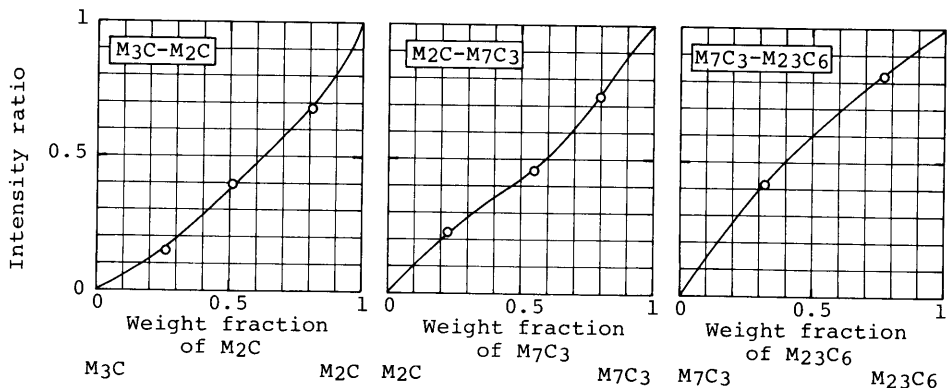


Fig.2 Cariblation curves between the ratio of diffracted beam intensity and weight fraction of carbide for  $M_3C-M_2C$ ,  $M_2C-M_7C_3$  and  $M_7C_3-M_{23}C_6$

### 3.3 Electron microscopic observations and electron beam diffraction of carbides

#### 3.3.1 Preparation of replicas

The electrolytic extraction—X-ray diffraction is the most suitable experimental method for the identification and quantitative analysis of carbides in steels. But this method is not sufficient to examine the shapes and distribution of carbides. And it is generally difficult to obtain the X-ray diffraction pattern by the very fine carbides in the earlier stage of precipitation. Then, the electron microscopic observations were carried out on the specimens quenched and tempered at various temperatures.

The extracted replicas were made by the following two methods.

Method I ---- The single-stage technique(Direct carbon replica technique)

(a) The specimen surface is polished and etched by 5 to 10% nital so that the microstructure is readily visible under the optical microscope. (b) A thin carbon film is evaporated directly on to the surface. (c) The carbon film is scored into small squares whilst it is still on the specimen. (d) The specimen is dipped into 15 to 25% nital for 1 hour. During chemical etching the squares of carbon film, on which the carbides are extracted, float into the nital. The separated squares are washed by acetone and distilled water, and then fixed on a grid.

Method II ---- The two-stage technique

(a) The specimen surface is polished and etched same as method I. (b) The first-stage replica is made by the acetylcellulose film. The carbides on the specimen surface are extracted mechanically on this film. (c) The second-stage carbon replica is made from the first-stage replica. The extracted carbides are transferred from the first-stage replica to the second-stage replica.

## 3.3.2 Determination of the diffraction constants for the electron microscope

The wave length of electron beam,  $\lambda$  is given by the following equation.

$$\lambda = \frac{h}{(2m_0 eE)^{\frac{1}{2}} (1 + \frac{eE}{2m_0 c^2})^{\frac{1}{2}}} \quad (\text{\AA})$$

$$= \frac{12.26}{E^{\frac{1}{2}} (1 + 0.9788 \cdot 10^{-6} E)^{\frac{1}{2}}}$$

h : Planck's constant  
 $m_0$  : mass of electron  
 e : charge of electron  
 c : light velocity  
 E : acceleration voltage

In the case of selected area diffraction, the carbide on the replica diffracts the electron beam. And the Bragg's law is formed. That is,

$$2d \sin\theta = \lambda$$

d : spacing of the reflecting lattice plane  
 $\theta$  : Bragg's angle

As shown in Fig.3, a lattice plane of carbide crystal diffracts the electron beam, and this diffracted beam gives a diffracted spot on the film. In the case of electron beam diffraction, the wave length is very short in comparison with the spacing of a lattice plane. Therefore Bragg's law can be rewritten as follows approximately.

$$dr = L\lambda$$

r : distance between the main spot and the diffracted spot  
 L : distance between the specimen and the film

Diffraction constants,  $L\lambda$  of the electron microscope (Hitachi H-700H) were determined using the evaporated film of copper as shown in Table 2.

If many particles of mono type carbide are present together in the selected area, the diffracted beam forms Debye-Scherrer rings as shown in Photo.1. The spacings of lattice planes can be calculated from the radii of the rings. While if the diffracting particle is the single crystal, the diffracted beam forms Laue pattern as shown in Photo.2. In this case, the spacing of the lattice plane

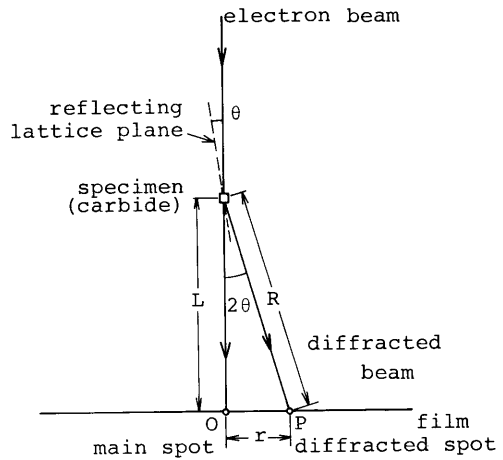


Fig.3 Electron beam diffraction

Table 2 Diffraction constants,  $L\lambda$  (mm $\cdot\text{\AA}$ )

acceleration voltage (kV)	electron diffraction camera length control (C.L.)				
	1	2	3	4	5
75	12.70	21.74	44.10	60.81	80.49
100	11.00	18.90	38.58	52.25	68.92
150	8.69	15.00	30.17	41.32	54.60
175	8.26	14.16	28.54	38.76	49.28
200	6.93	12.42	25.13	34.69	40.23

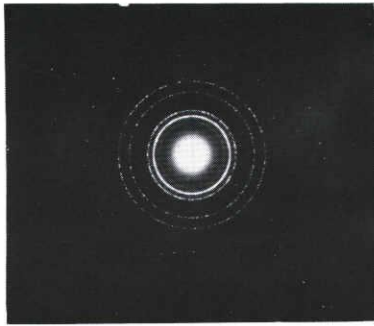


Photo.1 Debye-Scherrer rings  
obtained by many particles  
of mono type carbide

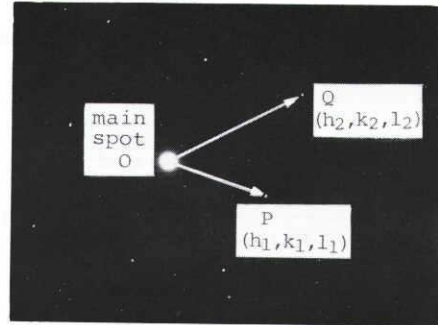


Photo.2 Laue pattern obtained  
by single crystal

Table 3 Carbide types formed in tempered Cr-Mo steels determined by  
X-ray analyses

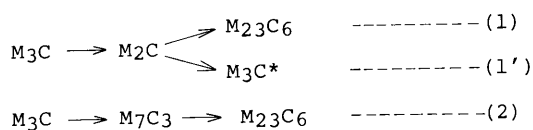
steel			tempering temperature and time								
No	%Mo	%Cr	500°C		600°C			700°C			
			24 hr	100hr	1 hr	5 hr	24 hr	100hr	1 hr	24 hr	100hr
A-0	0.5	0	M <sub>3</sub> C	n.p.	M <sub>3</sub> C	M <sub>3</sub> C M <sub>2</sub> C	M <sub>2</sub> C M <sub>3</sub> C	M <sub>2</sub> C M <sub>3</sub> C	M <sub>3</sub> C	M <sub>2</sub> C	M <sub>2</sub> C
A-1		0.6	n.p.		M <sub>3</sub> C	M <sub>3</sub> C M <sub>2</sub> C	M <sub>2</sub> C M <sub>3</sub> C	M <sub>2</sub> C M <sub>3</sub> C	M <sub>3</sub> C	M <sub>3</sub> C	M <sub>3</sub> C
A-2		1.1	M <sub>3</sub> C	n.p.	M <sub>3</sub> C		M <sub>2</sub> C M <sub>3</sub> C M <sub>7</sub> C <sub>3</sub>	M <sub>2</sub> C M <sub>3</sub> C M <sub>7</sub> C <sub>3</sub>	M <sub>3</sub> C	M <sub>3</sub> C M <sub>7</sub> C <sub>3</sub> M <sub>2</sub> 3C <sub>6</sub>	M <sub>3</sub> C M <sub>7</sub> C <sub>3</sub> M <sub>2</sub> 3C <sub>6</sub>
A-3		1.8	M <sub>3</sub> C	M <sub>3</sub> C M <sub>7</sub> C <sub>3</sub>	M <sub>3</sub> C	M <sub>7</sub> C <sub>3</sub> M <sub>3</sub> C	M <sub>7</sub> C <sub>3</sub>	M <sub>7</sub> C <sub>3</sub>	M <sub>3</sub> C M <sub>7</sub> C <sub>3</sub>	M <sub>7</sub> C <sub>3</sub> M <sub>2</sub> 3C <sub>6</sub>	M <sub>7</sub> C <sub>3</sub> M <sub>2</sub> 3C <sub>6</sub>
A-4		2.6	n.p.	M <sub>7</sub> C <sub>3</sub>	M <sub>7</sub> C <sub>3</sub>	M <sub>7</sub> C <sub>3</sub> M <sub>2</sub> 3C <sub>6</sub>	M <sub>7</sub> C <sub>3</sub> M <sub>2</sub> 3C <sub>6</sub>	M <sub>7</sub> C <sub>3</sub> M <sub>2</sub> 3C <sub>6</sub>	M <sub>7</sub> C <sub>3</sub> M <sub>2</sub> 3C <sub>6</sub>	M <sub>7</sub> C <sub>3</sub> M <sub>2</sub> 3C <sub>6</sub>	M <sub>7</sub> C <sub>3</sub> M <sub>2</sub> 3C <sub>6</sub>
A-5		5.3	M <sub>7</sub> C <sub>3</sub> M <sub>2</sub> 3C <sub>6</sub>	M <sub>7</sub> C <sub>3</sub> M <sub>2</sub> 3C <sub>6</sub>	M <sub>7</sub> C <sub>3</sub>	M <sub>7</sub> C <sub>3</sub> M <sub>2</sub> 3C <sub>6</sub>	M <sub>7</sub> C <sub>3</sub> M <sub>2</sub> 3C <sub>6</sub>	M <sub>7</sub> C <sub>3</sub> M <sub>2</sub> 3C <sub>6</sub>	M <sub>7</sub> C <sub>3</sub> M <sub>2</sub> 3C <sub>6</sub>	M <sub>2</sub> 3C <sub>6</sub>	M <sub>2</sub> 3C <sub>6</sub>
B-0		0	n.p.	n.p.	M <sub>2</sub> C		M <sub>2</sub> C M <sub>3</sub> C	M <sub>2</sub> C	M <sub>2</sub> C M <sub>3</sub> C	M <sub>2</sub> C M <sub>3</sub> C*	M <sub>2</sub> C M <sub>3</sub> C*
B-1	0.5	n.p.	n.p.	M <sub>2</sub> C M <sub>3</sub> C	M <sub>2</sub> C M <sub>3</sub> C	M <sub>2</sub> C M <sub>3</sub> C	M <sub>2</sub> C	M <sub>2</sub> C M <sub>3</sub> C	M <sub>2</sub> C M <sub>3</sub> C		
B-2	1.1	n.p.	n.p.	M <sub>2</sub> C M <sub>3</sub> C	M <sub>2</sub> C M <sub>3</sub> C	M <sub>2</sub> C M <sub>3</sub> C	M <sub>2</sub> C M <sub>3</sub> C M <sub>7</sub> C <sub>3</sub>	M <sub>2</sub> C M <sub>3</sub> C	M <sub>2</sub> C M <sub>3</sub> C M <sub>2</sub> 3C <sub>6</sub> M <sub>7</sub> C <sub>3</sub>		
B-3	1.4	n.p.	n.p.	M <sub>2</sub> C M <sub>3</sub> C	M <sub>2</sub> C M <sub>7</sub> C <sub>3</sub>	M <sub>2</sub> C M <sub>7</sub> C <sub>3</sub>	M <sub>7</sub> C <sub>3</sub> M <sub>2</sub> C	M <sub>7</sub> C <sub>3</sub> M <sub>2</sub> 3C <sub>6</sub>	M <sub>2</sub> 3C <sub>6</sub>		
B-4	2.0	n.p.	n.p.	M <sub>2</sub> C M <sub>3</sub> C		M <sub>7</sub> C <sub>3</sub> M <sub>2</sub> C M <sub>2</sub> 3C <sub>6</sub>	M <sub>7</sub> C <sub>3</sub> M <sub>2</sub> 3C <sub>6</sub>	M <sub>7</sub> C <sub>3</sub> M <sub>2</sub> 3C <sub>6</sub>	M <sub>2</sub> 3C <sub>6</sub>		
B-5	4.3	n.p.	n.p.	M <sub>7</sub> C <sub>3</sub> M <sub>2</sub> 3C <sub>6</sub>	M <sub>2</sub> 3C <sub>6</sub> M <sub>7</sub> C <sub>3</sub>	M <sub>2</sub> 3C <sub>6</sub>	M <sub>2</sub> 3C <sub>6</sub>	M <sub>2</sub> 3C <sub>6</sub>	M <sub>2</sub> 3C <sub>6</sub>		

n.p. : No diffraction pattern was obtained.

can be calculated from the distance between the main spot to the diffracted spot. And the crystal structure of carbide and Miller indices of the spots are determined. The vectors of OP and OQ in Photo.2 are equal to the reciprocal vectors of the lattice planes;  $(h_1, k_1, l_1)$  and  $(h_2, k_2, l_2)$  which reflect the spots of P and Q respectively. Therefore the angle between spot P and spot Q from main spot O is the angle between the two lattice planes of  $(h_1, k_1, l_1)$  and  $(h_2, k_2, l_2)$ .

#### 4. Sequences of carbide precipitation during tempering

Results of X-ray analyses on the extracted carbides are shown in Table 3. The following two types of sequences are recognized on the progress of tempering, that is elevating the temperature and passing the time.



$\text{M}_2\text{C}$  precipitation ( $\text{M}_3\text{C} \longrightarrow \text{M}_2\text{C}$ ), which is the first step of carbide reactions (1) or (1'), was recognized in steels containing relatively smaller chromium.  $\text{M}_2\text{C}$  carbide was transferred to  $\text{M}_{23}\text{C}_6$  generally. But the carbide reaction (1') ( $\text{M}_2\text{C} \longrightarrow \text{M}_3\text{C}^*$ ) was recognized in only 0%Cr-1%Mo steel, which had high Mo/C content ratio and low Cr/Mo content ratio.

Carbide reaction (2) was recognized in steels containing high chromium. In the high chromium steels the molybdenum carbide  $\text{M}_2\text{C}$  was not recognized.

In the steels, which had medium chromium content (1.1%Cr-0.5%Mo steel and 1.1 to 2.0%Cr-1%Mo steels), both carbide reactions (1) and (2) occurred simultaneously.

#### 5. Carbide morphologies observed by electron microscope

$\text{M}_3\text{C}$  carbide generally precipitates from martensite after the formation of  $\epsilon$ -carbide at the earlier stage of tempering. But in many Cr-Mo steels,  $\text{M}_3\text{C}$  carbide is already present in bainite structure under as-quenched condition. Fine  $\text{M}_3\text{C}$  carbide precipitating in bainite structure is shown in Photo.3 for as-quenched 1.1%Cr-0.5%Mo steel.  $\text{M}_3\text{C}$  carbides precipitated also on the lath boundaries of martensite in the same steel as shown in Photo.4-(a). The shape of this  $\text{M}_3\text{C}$  carbide is large film-like. Fine  $\text{M}_3\text{C}$  carbides in bainite structure remained up to the tempering temperature of 600°C. While, large film-like  $\text{M}_3\text{C}$  carbide grew with the progress of the tempering as shown in Photo.4-(b).

$\text{M}_7\text{C}_3$  carbides were recognized in 1.1%Cr-0.5%Mo steel tempered at 600°C for 5 hours as shown in Photo.5-(a).  $\text{M}_7\text{C}_3$  carbides were fine rod-like carbides. Photo.5-(b) was the Debye-Scherrer rings obtained from the selected area shown by the circle in Photo.5-(a). Diffraction pattern of  $\text{M}_3\text{C}$  was also superimposed on that of  $\text{M}_7\text{C}_3$  in the photograph.

$\text{M}_2\text{C}$  carbides precipitated uniformly in both grain interior and grain boundary.  $\text{M}_2\text{C}$  carbides were fine needle-like in shape as shown in Photo.6, which was the micrograph of 1.1%Cr-0.5%Mo steel tempered at 600°C for 5 hours. Photo. 7 also shows needle-like  $\text{M}_2\text{C}$  carbide present in 0%Cr-1%Mo steel tempered at

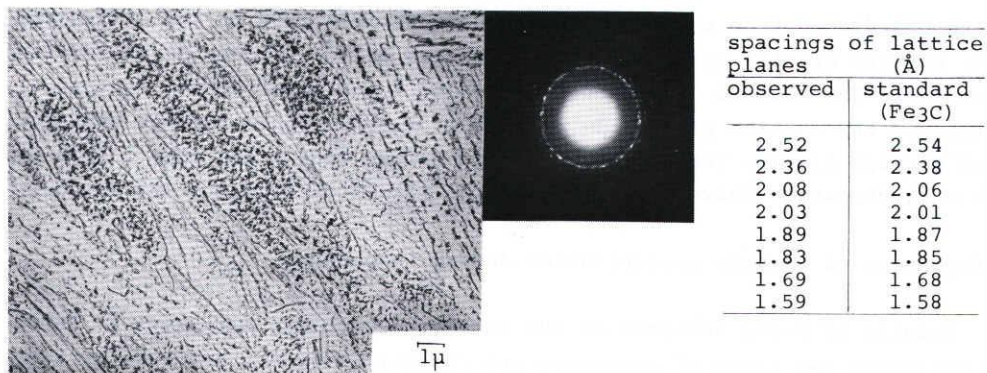


Photo.3 Electron micrograph of extracted replica taken from as-quenched 1.1%Cr-0.5%Mo steel showing the fine M<sub>3</sub>C carbides precipitating in bainite structure

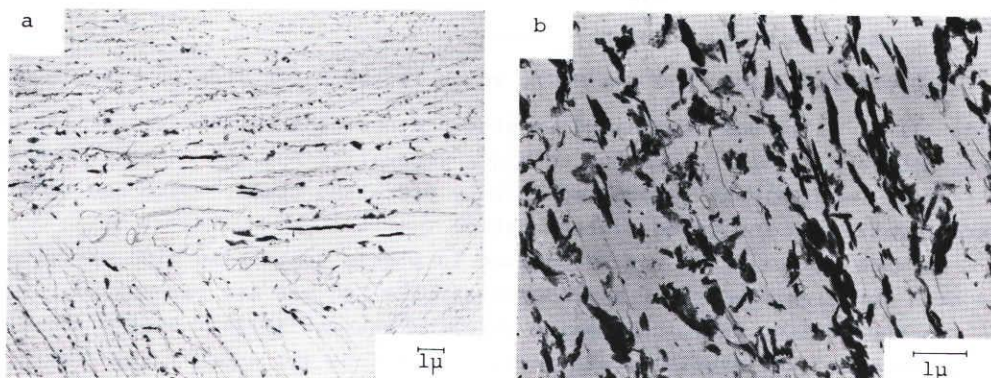


Photo.4 Electron micrographs of extracted replicas taken from 1.1%Cr-0.5%Mo steel showing the large film-like M<sub>3</sub>C carbides precipitating on the martensite lath boundaries (a)as-quenched (b) tempered at 550°C

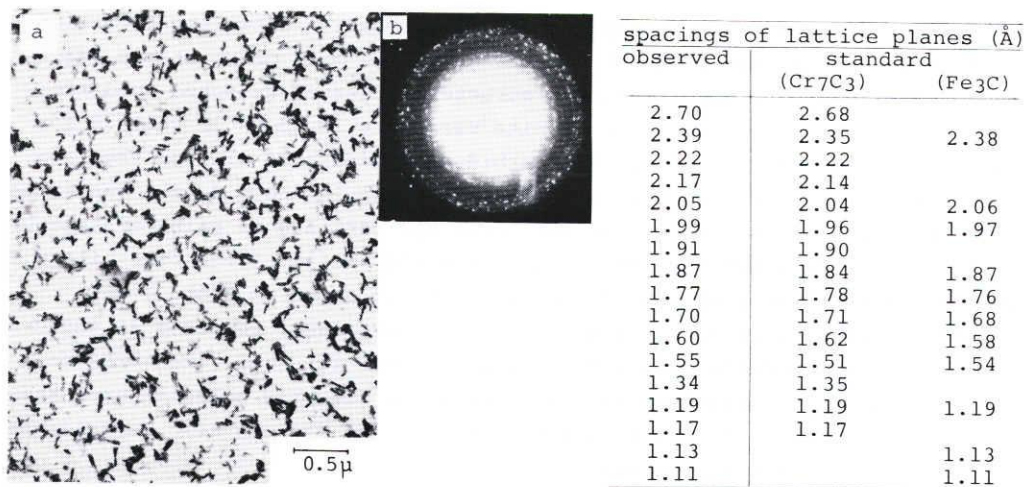


Photo.5 Electron micrograph of extracted replica taken from 1.1%Cr-0.5%Mo steel tempered at 600°C for 5 hours showing the fine rod-like carbides (a), and diffraction pattern by these carbides (b)

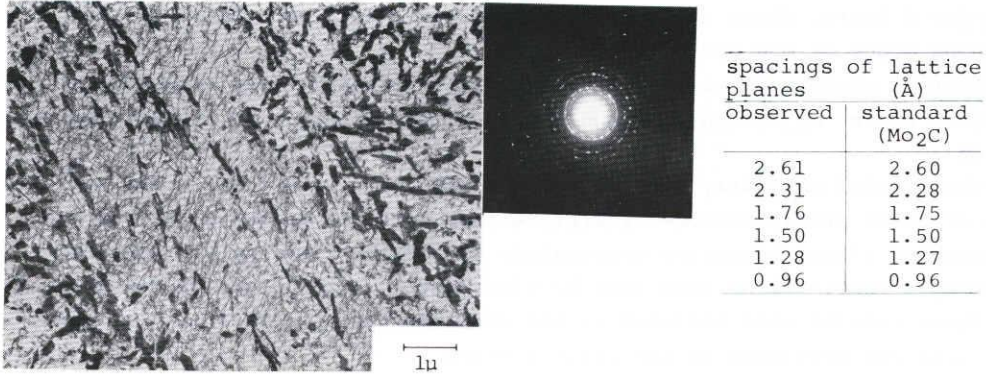


Photo.6 Electron micrograph of extracted replica taken from 1.1%Cr-0.5%Mo steel tempered at 600°C for 5 hours showing the fine needle-like M<sub>2</sub>C

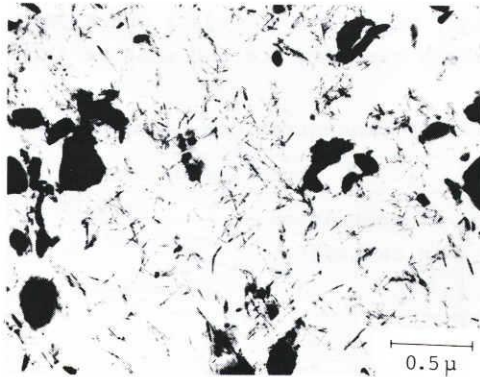


Photo.7 Electron micrograph of extracted replica taken from 0%Cr-1%Mo steel tempered at 600°C for 5 hours showing the needle-like M<sub>2</sub>C carbide

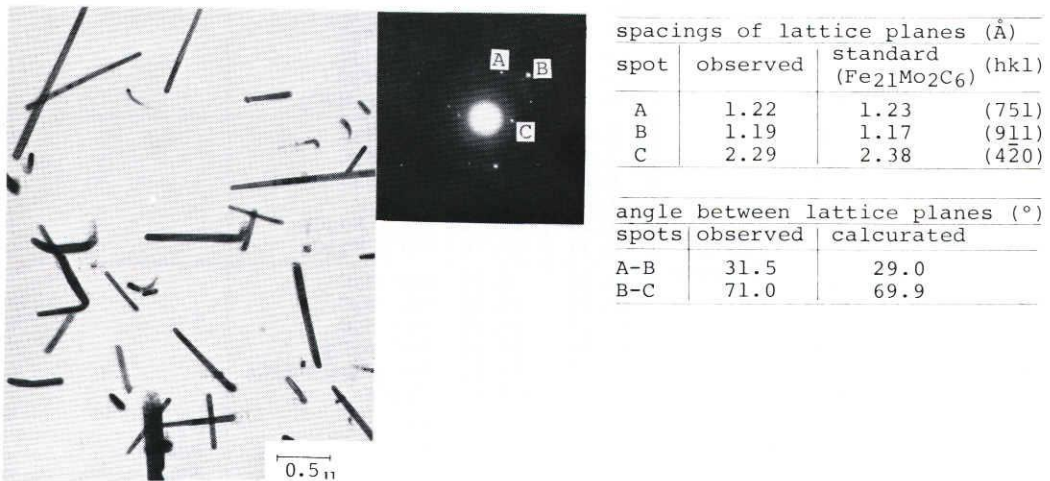


Photo.8 Electron micrograph of extracted replica taken from 4.3%Cr-1%Mo steel showing the large rod-like M<sub>23</sub>C<sub>6</sub> carbide

600°C for 5 hours. These needle-like  $M_2C$  carbides were recognized in the beginning stage of  $M_2C$  precipitation.

Photo.8 shows  $M_{23}C_6$  carbides present in 4.3%Cr-1%Mo steel tempered at 600 °C for 24 hours.  $M_{23}C_6$  carbide was also rod-like in shape and larger than  $M_7C_3$  carbide .

The special carbides, such as  $M_2C$  and  $M_7C_3$  were very fine at the beginning stage of their precipitations. Therefore they were recognized at earlier stage of tempering (lower tempering temperature or shorter time) by the electron microscopic examinations than that by electrolytic extraction and X-ray analysis. These results were included as the complementary plots of the carbide phase diagrams mentioned in the later section.

#### 6. Chemical analyses of extracted carbides

Although the lattice structure of the carbides found in tempered Cr-Mo steels are same as those of  $Fe_3C$ ,  $Mo_2C$ ,  $Cr_7C_3$ ,  $Cr_{23}C_6$  and  $Fe_2MoC$ , respectively, the chemical compositions of those carbides are not same as that calculated

Table 4 Chromium and molybdenum concentrations of extracted carbides

No	steel		tempering temperature and time	extracted carbide			
	content in steel (%)			concentration in carbide (%)		carbide type	
	Mo	Cr		Mo	Cr	determined by X-ray diffraction	estimated from chemical analysis
A-0	0.5	0	600°C 1 hour	5.53	0.40		$M_2C$
A-1		0.6		4.53	4.39	$M_3C$	$M_2C$
A-2		1.1		5.58	10.95	$M_3C$	$M_2C$
A-3		1.8		4.87	16.61	$M_3C$	
A-4		2.6		3.55	22.96	$M_7C_3$	
A-5		5.3		3.58	39.35	$M_7C_3$	
B-0	1	0	600°C 1 hour	10.00	0.43	$M_2C$	
B-1		0.5		18.10	3.48	$M_2C$ $M_3C$	
B-2		1.1		23.00	8.25	$M_2C$ $M_3C$	
B-3		1.4		13.28	16.15	$M_2C$ $M_3C$	
B-4		2.0		10.38	22.96	$M_2C$ $M_3C$	
B-5		4.3		7.18	44.68	$M_{23}C_6$ $M_7C_3$	
A-0	0.5	0	600°C 24 hours	8.40	0.16	$M_2C$ $M_3C$	
A-1		0.6		7.48	12.04	$M_2C$ $M_3C$	
A-2		1.1		6.20	16.11	$M_2C$ $M_3C$ $M_7C_3$	
A-3		1.8		4.22	33.50	$M_7C_3$	
A-4		2.6		3.30	46.48	$M_7C_3$ $M_{23}C_6$	
A-5		5.3		3.34	55.70	$M_7C_3$ $M_{23}C_6$	
B-0	1	0	600°C 24 hours	29.30	0.99	$M_2C$ $M_3C$	
B-1		0.5		26.10	10.02	$M_2C$ $M_3C$	
B-2		1.1		25.25	19.68	$M_2C$ $M_3C$	
B-3		1.4		20.60	24.26	$M_2C$ $M_7C_3$	
B-4		2.0		9.30	42.32	$M_7C_3$ $M_2C$ $M_{23}C_6$	
B-5		4.3		17.55	64.06	$M_{23}C_6$	
A-0	0.5	0	700°C 1 hour	5.33	0.0	$M_3C$	$M_2C$
A-1		0.6		6.86	6.28	$M_3C$	$M_2C$
A-2		1.1		3.54	16.23	$M_3C$	$M_7C_3$
A-1	0.5	0.6	700°C 24 hours	2.97	13.79	$M_3C$	$M_7C_3$
			700°C 100 hours	-	16.65	$M_3C$	$M_7C_3$

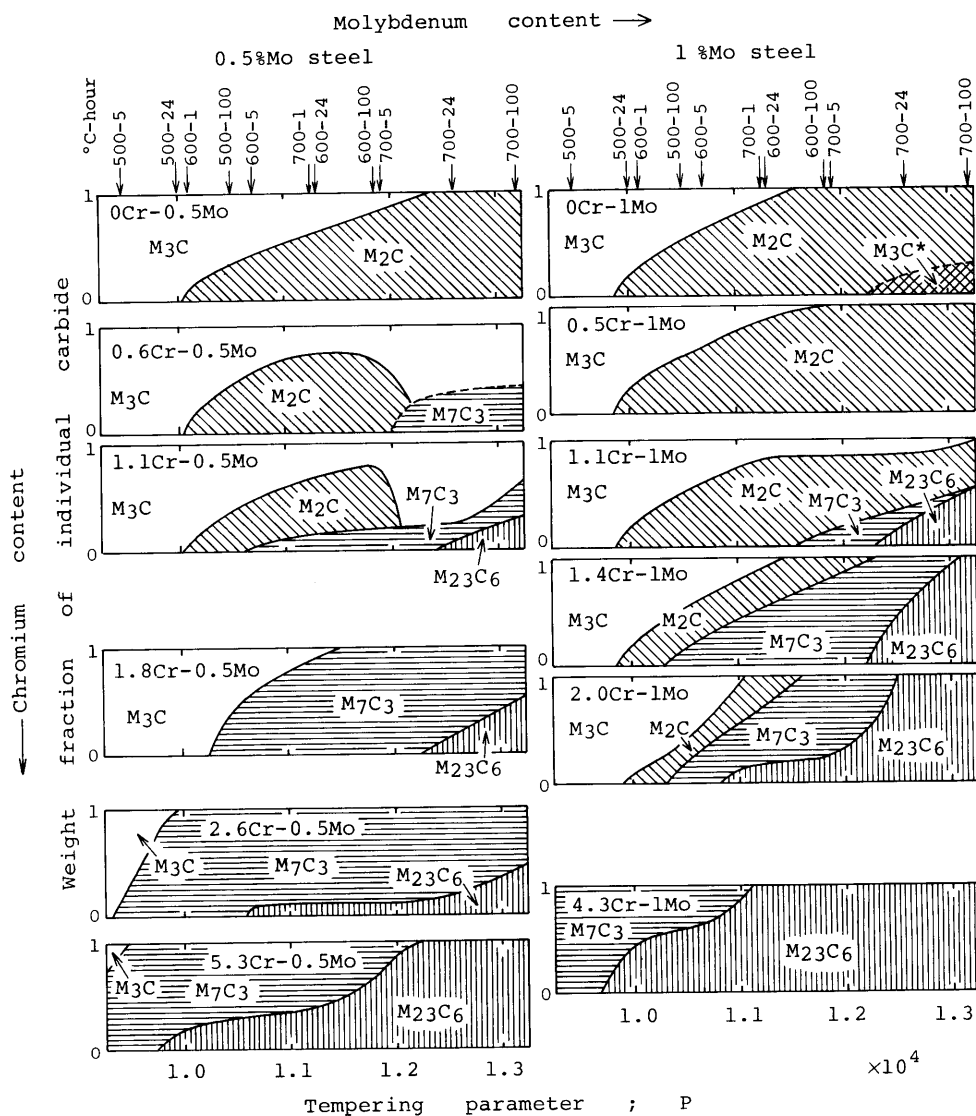


Fig.4 Weight fraction of the individual carbide extracted from tempered Cr-Mo steels

from such the chemical formulas, because those carbides contain iron, molybdenum or chromium as solid solution. Therefore chemical analyses of chromium and molybdenum were carried out on the extracted carbides according to the standard methods of J.I.S.. Because the decomposition of carbides was difficult by the acid recommended by J.I.S., the following mixed acid was used.

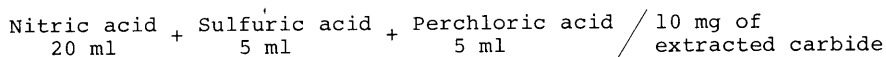


Table 4 shows the concentrations of chromium and molybdenum in extracted carbides.

According to the ternary equilibrium phase diagrams of Fe-C-Cr and Fe-Mo-C, the solubilities of chromium and molybdenum in  $M_3C$  carbide are 15 and 3wt%,

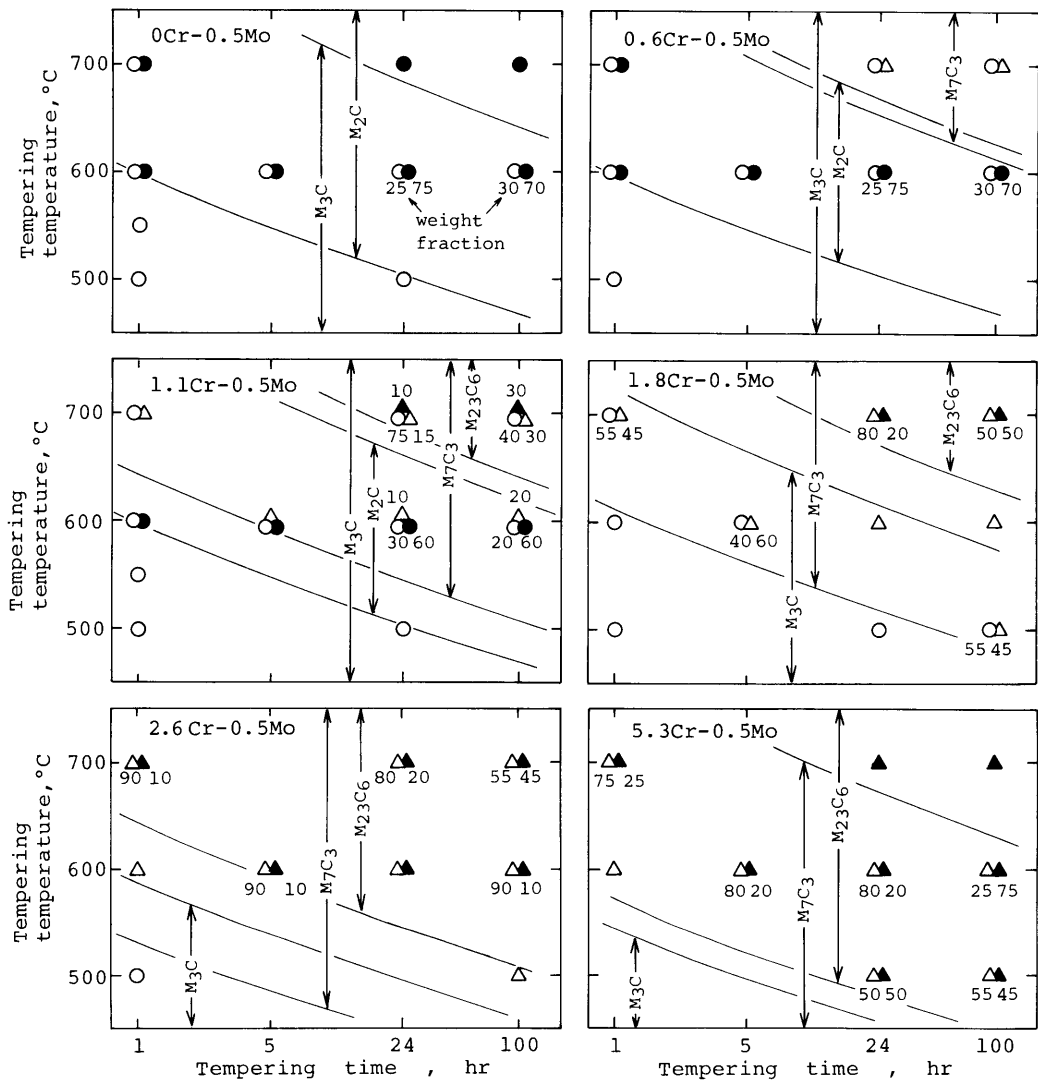


Fig.5 Carbide phase diagrams of Cr-0.5%Mo steels during tempering

Note; ○M<sub>3</sub>C ●M<sub>2</sub>C △M<sub>7</sub>C<sub>3</sub> ▲M<sub>23</sub>C<sub>6</sub>

respectively. Therefore, the M<sub>3</sub>C carbide specimen containing larger chromium or molybdenum than each solubility can be considered the mixture of M<sub>3</sub>C-M<sub>7</sub>C<sub>3</sub> or M<sub>3</sub>C-M<sub>2</sub>C. Carbide types estimated from chemical analyses are shown in Table 4.

#### 7. Carbide phase diagrams of Cr-Mo steels during tempering

Because the carbide reaction (carbide phase change) in steel are caused by the diffusions of carbon and other alloying elements, such as chromium and molybdenum, it is thought that the progress of carbide reaction is expressed by the tempering parameter; P defined by the following equation.

$$P = T(\log t + c)$$

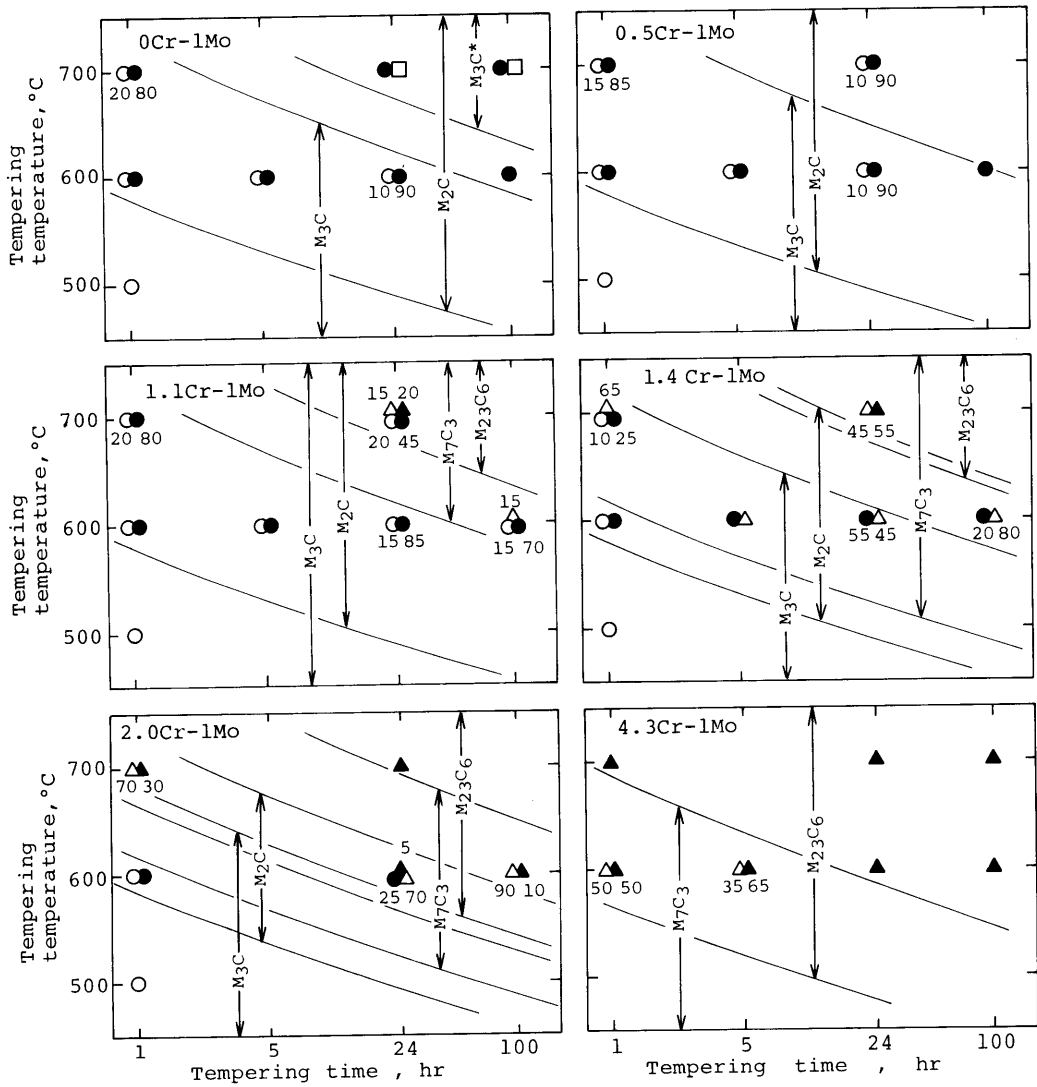


Fig.6 Carbide phase diagrams of Cr-1%Mo steels during tempering

Note; ○  $M_3C$  ●  $M_2C$  △  $M_7C_3$  ▲  $M_{23}C_6$  □  $M_3C^*$

T : tempering temperature (°K)

t : tempering time (sec)

c : constant which is dependent on the material

The value of constant, c is altered by the chemical compositions of the steel. In this study, the constant, c was found to be about eight.

Fig.4 shows the weight fraction of the individual carbide for each Cr-Mo steel using the tempering parameter as the abscissa. From this figure the followings can be pointed.

- (i) In the chromium free or low chromium steels,  $M_2C$  carbide dominantly precipitated.
- (ii) As the chromium content was increased, the precipitation regions of  $M_7C_3$

carbide expressed by tempering parameter, P extended and the precipitation time was advanced.

- (iii) As the molybdenum content was increased, the precipitation region of  $M_2C$  carbide extended. Conversely the precipitation of the chromium carbide  $M_7C_3$  was suppressed.
- (iv)  $M_{23}C_6$  carbide was stabilized not only by increasing chromium content but also by increasing molybdenum content.

Fig.5 and Fig.6 show the carbide phase diagrams of Cr-0.5%Mo and Cr-1%Mo steels respectively. The plots in these figures included the results of X-ray analyses, electron microscopic observation and chemical analyses of extracted carbides. The tempering temperature-time regions were divided by some curved lines at which the each carbide precipitated and disappeared.

## 8. Conclusions

Precipitation of carbides during tempering were investigated for the Cr-Mo steels of 0 to 5%Cr and 0.5 to 1%Mo. A series of experimental method, which consisted of electron beam diffraction on extracted replica, X-ray diffraction and chemical analysis on extracted carbide, and electron microscopic observation, was established in order to confirm the carbide phase change in Cr-Mo steels. The results are summarized as follows.

- (1) Carbide phase change(carbide reaction),  $M_3C \rightarrow M_2C \rightarrow M_{23}C_6$  or  $M_3C^*$  was found in 0 to 1.1%Cr-0.5%Mo and 0 to 2.0%Cr-1%Mo steels. And the other carbide phase change,  $M_3C \rightarrow M_7C_3 \rightarrow M_{23}C_6$  was found in 0.6%Cr-0.5%Mo and 1.1 to 4.3%Cr-1%Mo steels. Both the carbide phase changes were recognized in 0.6 to 1.1%Cr-0.5%Mo and 1.1 to 2.0%Cr-1%Mo steels
- (2) The sequence of carbide precipitation in each Cr-Mo steel was described in the carbide phase diagram shown in the tempering temperature-time diagram.

## Acknowledgments

The present investigation has been supported by The Grant-in-Aid in 1979 for Scientific Research of The Ministry of Education and Culture.

The electron microscopic examination in this study were carried out in The Electron Microscope Center, Mie University.

The authors wish to thank Mr.M.Marui, Mr.Y.Nakaseko, Mr.M.Tajiri and Mr.S. Adachi in Faculty of Engineering, Mie University for their cooperative works.

## References

- 1)K.Tamaki and J.Suzuki: Research Rep. Fac. Eng.,Mie Univ.,6,51-62(1981).
- 2)K.Bungardt et al.: Arch. Eisenhütt.,29,193(1958).
- 3)T.Sato and T.Nishizawa: J.Inst.Metals.Japan,24,473-477(1960) [in Japanese].
- 4)T.Sato,T.Nishizawa and K.Tamaki: *ibid.*,24,395-399(1960) [in Japanese].
- 5)T.Takei: Kinzoku no Kenkyu,9,163(1932)[in Japanese].
- 6)D.J.Dyson and K.W. Andrews: J.Iron and Steel Inst.,202,325-329(1964).
- 7)K.W.Andrews,H.Hughes and D.J.Dyson: *ibid.*,210,337-350(1972).
- 8)W.Jellinghaus: Arch.Eisenhütt.,42,133(1971).